Covalent 2D Patterning, Local Electronic Structure and Polarization Switching of Graphene at the Nanometer Level

Lipiao Bao,[a] Baolin Zhao,[b] Mhamed Assebban,[a] Marcus Halik,[b] Frank Hauke,[a] and Andreas Hirsch*[a]

Abstract: A very facile and efficient protocol for the covalent patterning and properties tuning of graphene is reported. Highly reactive fluorine radicals were added to confined regions of graphene directed by laser writing on graphene coated with 1-fluoro-3,3-dimethylbenziodoxole. This process allows for the realization of exquisite patterns on graphene with resolutions down to 200 nm. The degree of functionalization, ranging from the unfunctionalized graphene to extremely high functionalized graphene, can be precisely tuned by controlling the laser irradiation time. Subsequent substitution of the initially patterned fluorine atoms afforded an unprecedented graphene nanostructure bearing thiophene groups. This substitution led to a complete switch of both the electronic structure and the polarization within the patterned graphene regions. This approach paves the way towards the precise modulation of the structure and properties of nanostructured graphene.

Well-controlled fabrication and properties modulation of 2D graphene nanoarchitectures remain quite challenging, despite their highly attractive potential in high-tech application fields like electronics, catalysis, and sensors.[1–4] Realization of this goal relies on the disclosure of facile and efficient chemical approaches to anchor/switch functional groups on graphene in a well-defined order to engineer the structure and surface properties of graphene. In preceding reports, five methods for graphene patterned functionalization have been reported, namely, poly(methyl methacrylate) (PMMA)-assisted lithography,[5–8] laser/plasma writing,[9–12] force-accelerated patterning,[13] space-controlling by self-assembly[14–16] and our recently developed 2D-substrate patterning.[17] The use of these methods led to examples of patterned graphene architectures bearing for instance atomic hydrogen and aryl addends.[6] Indeed, these initial results represent considerable progresses for the 2D-engineering of graphene. Yet, from a general perspective, precise and controllable 2D-patterning of graphene remains a very challenging task leaving a couple of crucial bottlenecks: I) functional groups applicable for graphene patterning are still very scarce – only hydrogen[6] and fluorine atoms,[9] diazonium salts,[6,14,15] *cis*-dienes,[7] cyclopentadienes,[13] and peroxides[11,12] have been patterned to selected regions of graphene; II) the degree of functionalization is generally on the one hand not easy to control and on the other hand relatively low in most cases being in the low-functionalization-regime of the Cançado curve.[18] Two exceptions are fluorination and trifluoromethylation which have been demonstrated to be efficient methods towards highly functionalized graphene;[9,17,19] III) whilst the 5 nm process have been commercially used for silicon-based electronics, the current resolution of covalent 2D-patterning of graphene is generally limited to the super-micrometer range. The only few exceptions are based on the implementation of scanning tunneling microscopes (STM) as a patterning tool, a technique which is highly difficult to handle and does not allow for the realization of arbitrary pattern designs in large areas.[20–22] Overcoming these drawbacks represents the next higher level of graphene 2D-engineering.

On the basis of the 2D-chemistry of graphene patterning, the next goal is to precisely manipulate the properties of graphene nanostructures for target demands through patterning/switching specific functional addends on graphene. However, research in this direction is still in its infancy and to the best of our knowledge, only three examples of electronic property alteration (fluorination,[9] photocycloaddition[16] and hydrogen desorption[20]) and two cases of surface potential modulation (diazonium[5] and Diels-Alder reaction[7]) of patterned graphene nanostructures have been reported so far. Moreover, all these preceding examples are limited to a single-step functionalization of graphene. For the realization of multi-functional graphene 2D-architectures useful for real applications like electronics, a multi-step manipulation of graphene's properties through a stepwise graphene chemistry is of vital importance but still unfulfilled.

Here, we report a new simplistic and highly efficient method for graphene fluorination in a patterned fashion, and for the first

[a] Dr. L. Bao, Dr. M. Assebban, Dr. F. Hauke, Prof. Dr. A. Hirsch
Department of Chemistry and Pharmacy & Joint Institute of Advanced Materials and Processes (ZMP)
Friedrich-Alexander University of Erlangen-Nürnberg
Nikolaus-Fiebiger-Strasse 10, 91058 Erlangen (Germany)
E-mail: andreas.hirsch@fau.de

[b] B. Zhao, Prof. Dr. M. Halik
Organic Materials and Devices (OMD), Institute of Polymer Material, Interdisziplinären Zentrums für Nanostrukturierte Filme (IZNF)
Friedrich-Alexander University of Erlangen-Nürnberg
Cauerstraße 3, 91058 Erlangen (Germany)

Supporting information for this article is available on the WWW under https://doi.org/10.1002/chem.202100941

time, the switching of the local electronic structure and polarization in confined areas of graphene at the nanometer level through a two-step treatment of graphene chemistry. Highly reactive fluorine radicals, generated by the decomposition of an environmental-friendly and mild fluorination reagent 1-fluoro-3,3-dimethylbenziodoxole (**FMBO**)[23,24] (Figure 1) under laser irradiation, were attached to the graphene surface in a spatially defined manner. The degree of functionalization – spanning from the unfunctionalized graphene to extremely functionalized graphene (in the high-functionalization-regime of the Cançado curve[18]) – can be precisely controlled by tuning the laser irradiation time. Compared to the reported fluorination of graphene using a fluoropolymer (CYTOP)[9] where both F and CF_x radicals are involved, our present work demonstrates that the usage of small molecule **FMBO** provides clear advantages: I) a more homogeneous functionalization nature with only F addends; II) a higher degree of functionalization at a faster reaction rate; III) the possibility of graphene patterning also in the liquid-phase, in addition to the common solid-state condition; IV) the post-patterning removal of the residual **FMBO** layer is very facile as opposed to the difficult removal of CYTOP on graphene which requires a special stripper but also a much longer time. Remarkably, the resolution of our protocol approaches the nanometer regime and exquisite pattern designs can easily be realized. In follow-up reactions, the fluorine atoms can be substituted by nucleophiles. While this substitution has provided plenty of room for patterning of otherwise difficult addends on graphene with very high degree of functionalization, it allows also for the precise properties engineering of graphene at the nanometer scale, as an example, doping and polarization switching has been demonstrated in this work.

Our patterning protocol illustrated in Figure 1 utilized the generation of highly reactive fluorine radicals of **FMBO** deposited on monolayer graphene under laser irradiation (see Supporting Information for the experimental details). For this purpose, a layer of **FMBO** was dip-coated onto a monolayer graphene supported by a SiO_2/Si wafer. Note that the use of a reactive SiO_2/Si substrate here is crucial as it permits a strain-free antaratopic addition mode through bottom-side quenching by the reactive supernatant SiO_2 layer on the substrate (Figure 1b), which could therefore allow for high degrees of functionalization.[17,25,26] Subsequently, the generated highly reactive fluorine radicals undergo covalent addition on the top surface of graphene. The generation of F radicals, which takes place only at the laser-irradiated area leads to a locally controlled functionalization of graphene. The laser irradiation can be nicely controlled and as a result, a sophisticated pattern (the logo of our SFB project, Figure 1c and S1) is demonstrated here. After the writing process, the residual reagent layer was removed by washing with THF, affording the patterned graphene sample denoted as **fG**.

The functionalization process was monitored *in situ* by Raman spectroscopy. Figure 2a depicts the Raman spectra of the graphene sample as a function of the laser irradiation time. The time study revealed that laser irradiation for only 0.2 s has already induced the appearance of a pronounced D-band, which correlates with the sp^3-hybridization of sp^2-lattice carbon due to the covalent attachment of F atoms onto graphene. After 1 s irradiation, an I_D/I_G ratio of 1.5 was observed and the 2D-band was significantly reduced ($I_{2D}/I_G = 1$ compared to $I_{2D}/I_G = 2$ for the pristine monolayer graphene). Higher degrees of functionalization can be achieved by simply increasing the laser

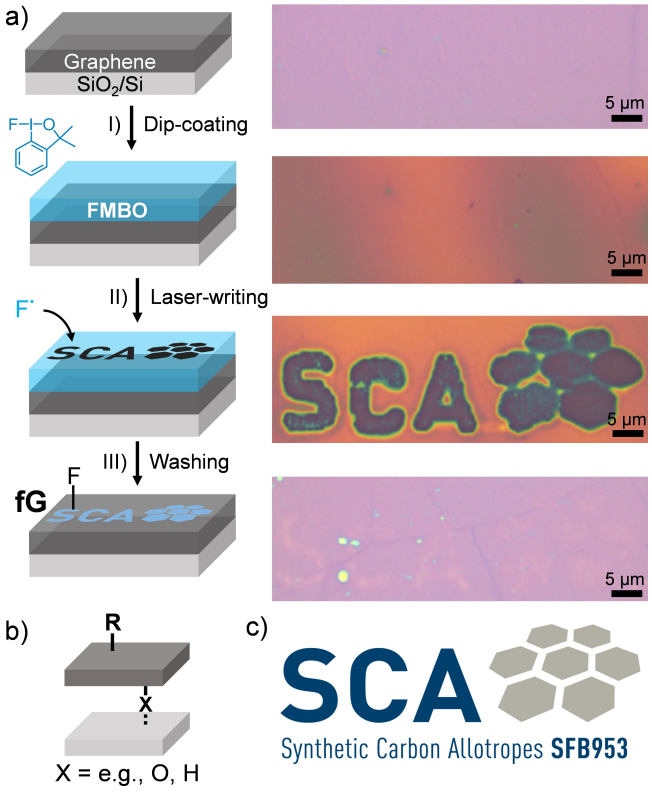

Figure 1. a) Schematic illustration of the laser writing process (left) and the corresponding microscopic images of the sample at each step (right): I) a layer of **FMBO** was dip-coated onto a monolayer graphene supported on a SiO_2/Si substrate. II) Laser writing with a green laser ($\lambda = 532$ nm, see Supporting Information for the detailed parameters) on predefined regions generated highly reactive F radical intermediates which subsequently added onto the graphene surface. III) The residual reagent layer was removed by THF, yielding the corresponding patterned graphene sample denoted as **fG**; b) the binding topology of the functionalized graphene of **fG** and **fG-Sub**; c) the pattern design (the logo of our SFB project of "Synthetic Carbon Allotropes") used in the laser writing process.

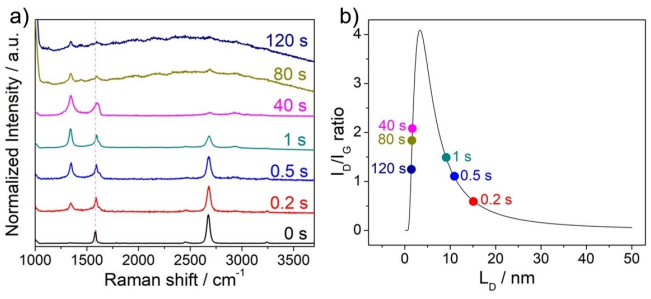

Figure 2. a) Raman spectrum of the monolayer graphene coated with **FMBO** as a function of laser irradiation time and b) the corresponding I_D/I_G profile located on the Cançado curve.[18] L_D: the mean distance between defects. The pink dashed line indicates the position of G-band (1582 cm^{-1}) of the starting monolayer graphene. $\lambda_{exc} = 532$ nm.

irradiation time. After 40 s, both the D- and G-band became very broad and the 2D-band almost vanished. This is a direct indication of a very high degree of functionalization which falls in the high-functionalization-regime of the Cançado curve (Figure 2b).[18] Further increase of the laser irradiation time to 120 s generated a Raman spectrum with broad fluorescence signal and very week characteristic D- and G-band of graphene, suggesting the formation of extremely high fluorinated graphene.[27] The increased functionalization degree correlates with the laser irradiation time. This goes also in line with the G-band upshift (Figure 2a) due to the attachment of electron-withdrawing F atoms in the functionalized regions.[27] For example, after laser irradiation of 40 s, the G-band is located at 1603 cm^{-1}, corresponding to an up-shift of 21 cm^{-1} compared to that of the starting graphene (1582 cm^{-1}). Significantly, the irradiation-based functionalization of SiO_2/Si supported monolayer graphene can also be conducted in the liquid phase where the degree of functionalization can correspondingly be precisely controlled by the time of laser irradiation (Figure S2).

Since the functionalization could be well-controlled both in terms of the region-selectivity and the degree of functionalization, patterned fluorination could be easily realized by our laser writing process. As a prototype, our 'SCA' logo (Figure 1c) was written on graphene and each point was irradiated for 40 s. The reaction steps can be visualized with the corresponding optical images of the sample (Figure 1). After laser treatment, the irradiated regions match well with our input pattern design (Figure 1c). Interestingly, in the optical image of the sample after washing, the input pattern could already be distinguished: the irradiated area shows higher transparency compared with the unreacted regions. This indicates the successful high degree of fluorination in the patterned area as fluorination increases the transparency of monolayer graphene according to the previous reports.[28] In Figure 3a the corresponding Raman mean spectra are depicted. For the non-irradiated area, an I_D/I_G ratio of <0.1 is found, confirming its undisturbed nature. In contrast, a 40 s irradiation at the patterned area has induced a very high degree of local fluorination, which is reflected by the very broad D- and G-bands but very weak 2D-band as well as the significant G-band shift (1603 cm^{-1} compared to 1582 cm^{-1} of the pristine graphene). Besides, the corresponding I_D/I_G ratio of these patterned areas exhibits a uniform distribution centered at around 2 (Figure 3b), further confirming the successful and uniform fluorination at these patterned areas.

To visualize this chemical pattern, a large-scale Raman mapping of the I_D/I_G ratio (60×20 μm^2) was performed. Clearly, our pattern design can be easily distinguished in the corresponding Raman I_D/I_G map (Figure 4a), which is in perfect agreement with the input pattern design and the optical image of the sample after washing (Figure 1a). In addition to the high accuracy of the laser pathway, our approach could provide a very high resolution down to ca. 200 nm. To verify this very important merit, parallel lines with perpendicular distances of 1 μm were written on graphene by laser irradiation (Figure 4b). After the removal of residual **FMBO**, the acquired Raman D-band map shown in Figure 4c confirms the very high resolution of ca. 200 nm. Such a nanometer scale resolution realized in this work constitutes a new level of covalent 2D-patterning of graphene.

The successful implementation of the chemical pattern on **fG** was further corroborated by Kelvin probe force microscopy (KPFM). First, the topographic scan using the conventional atomic force microscopic (AFM) showed no significant height variation (Figure 5a and 5c) between the patterned and unfunctionalized region. This could be explicitly rationalized by considering the surface contaminants and the length of the C–F bond (ca. 1.35 Å) which is in the same order as our AFM

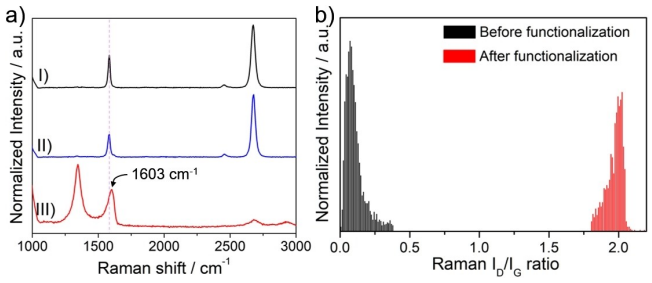

Figure 3. a) Mean Raman spectra of starting graphene (I), graphene regions without (II) and with laser irradiation (III). b) Statistical Raman I_D/I_G histogram of the functionalized areas of **fG** in comparison to the histogram obtained for the starting material. $\lambda_{exc}=532$ nm.

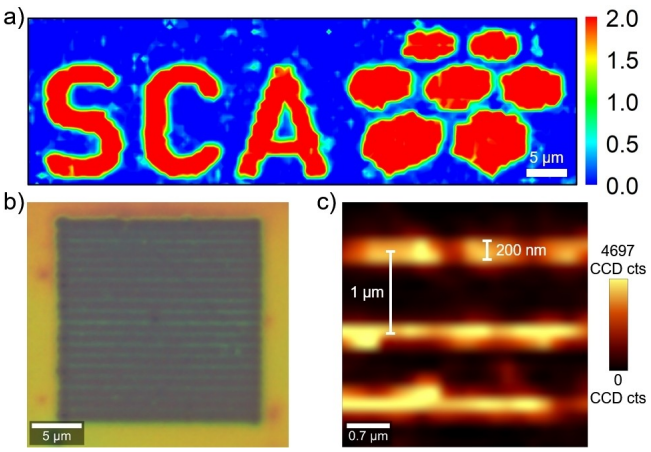

Figure 4. a) Raman I_D/I_G map of **fG**, b) optical image of the graphene sample after laser writing of parallel lines and c) Raman D-band map of the sample after the removal of **FMBO**. $\lambda_{exc}=532$ nm.

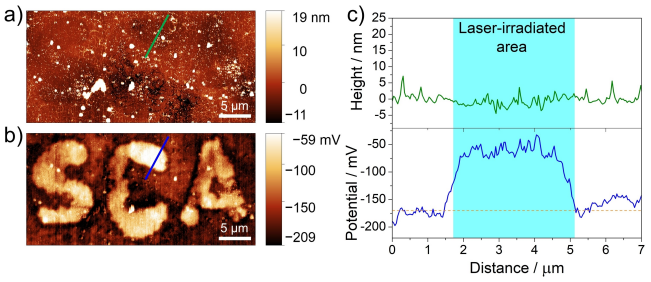

Figure 5. a) AFM and b) KPFM images of fG, c) height (green line, upper) and surface potential (blue line, lower) profiles of **fG**.

uncertainty limit (0.1 nm). Consequently, the chemical pattern is difficult to be distinguished from the AFM height scan (Figure 5a). In contrast, the pattern can be clearly visualized by KPFM (Figure 5b) and matches well with the input pattern design (Figure 1c) as well as the Raman I_D/I_G map of **fG** (Figure 4a). The functionalized area shows a higher surface electrostatic potential of ca. 120 mV (Figure 5c) compared to the undisturbed area, due to the very strong electron-withdrawing ability of covalently attached F atoms on graphene and the resulted p-doped nature of **fG** in the patterned area. This surface potential difference gives rise to stark contrast as proved by KPFM, thus yielding a clear image of the functionalized pattern (Figure 5b). Moreover, the surface potential line profile shows a sharp pattern edge (Figure 5c, bottom), which further confirm that very high resolution (ca. 200 nm) pattern can be realized by our laser writing process.

The thermal stability of the fluorinated graphene **fG** was investigated using temperature-dependent Raman spectroscopy. At 50 °C (Figure 6), the sample shows an I_D/I_G ratio of around 2 and a negligible 2D-band – as discussed above – which suggests a very high degree of functionalization falling in the high-functionalization-regime of the Cançado curve.[18] Very little change in the Raman spectra could be observed below 350 °C, suggesting a relatively high stability in this temperature range. Further increasing the temperature to 500 °C results in the complete disappearance of the characteristic Raman features (D-, G- and 2D-band) due to the complete destruction of the graphene framework as a consequence of the very high degree of fluorination within the functionalized sample **fG**.[17,29]

Another significant merit of our protocol is the combination of this facile patterned approach with the nucleophilic substitution reaction of fluorinated graphene.[30–32] Considering its simplicity, the nanometer scale resolution of our laser writing method and the wide variety of nucleophiles, the potential for patterning of otherwise difficult to bind addends with very high degree of functionalization and precise properties engineering at the nanometer level are very exciting. To verify this concept, **fG** was reacted with 3-thienylmagnesium iodide to substitute the fluorine addends with thiophene affording **fG-Sub** (Figure 7a). The corresponding Raman spectra before and after the substitution are shown in Figure 7b. The Raman spectrum of **fG-Sub** resembles that of **fG** (*e.g.*, comparable I_D/I_G and I_{2D}/I_G ratio),

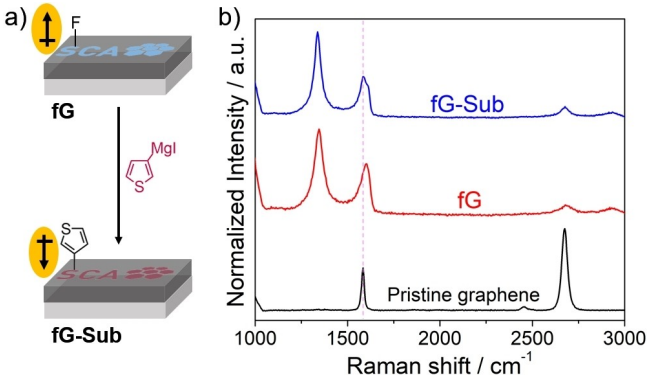

Figure 7. a) Schematic illustration of the substitution reaction of **fG** with 3-thienylmagnesium iodide affording **fG-Sub**, b) Raman spectra of the patterned area of the graphene sample before and after the substitution reaction. $\lambda_{exc} = 532$ nm. The arrows indicate the polarization of the graphene sample.

because the substitution does not change the sp^3-hybridized structure of graphene at the patterned area. However, the G-band of **fG-Sub** locates at 1582 cm^{-1} with a significant down-shift compared to that of **fG** (1603 cm^{-1}), indicating the successful substitution and fabrication of an unprecedented patterned graphene sample bearing thiophene groups.

Further solid proof for this substitution is provided by the KPFM result (Figure 8b) and the elemental distribution of S (Figure 8e) of **fG-Sub**. Both clearly show the 'SCA' pattern which is in excellent agreement with the input pattern design. Besides, the 'SCA' pattern can also be distinguished from the SEM image (Figure 8d), suggesting the distinct nature of the patterned areas compared to the unfunctionalized regions. In contrast to the case of **fG**, the surface potential of the patterned areas of **fG-Sub** is now lower by ca. 70 mV than that of non-patterned areas. This corresponds to a complete switch of both the doping (from p-doped to n-doped) and the polarization of our graphene nanostructure (Figure 7a), due to the substitution of the electron-withdrawing fluorine atoms with electron-donating thiophene groups. This complete switch of the doping and polarization,

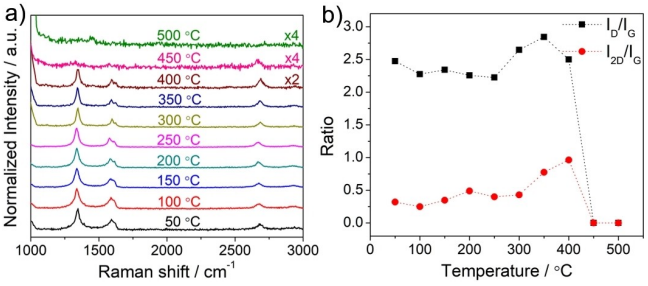

Figure 6. a) Temperature-dependent Raman spectra of **fG** and b) mean Raman I_D/I_G and I_{2D}/I_G ratios extracted from temperature-dependent Raman spectra. $\lambda_{exc} = 532$ nm. These Raman spectra have been zoomed for clarity.

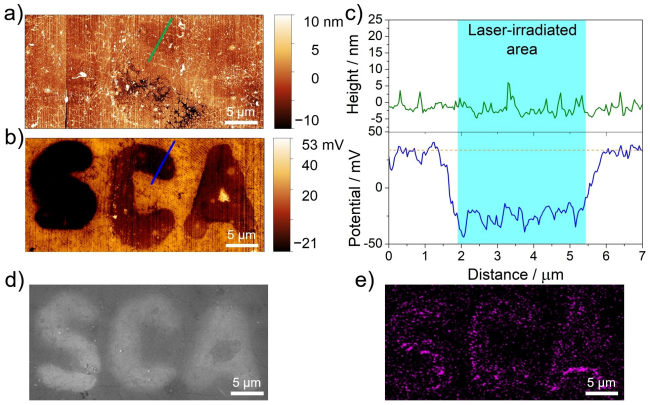

Figure 8. a) AFM and b) KPFM images of **fG-Sub**, c) height (green line, upper) and surface potential (blue line, lower) profiles of **fG-Sub**. d) SEM and e) S elemental mapping of **fG-Sub**.

combined with the Raman result (Figure 7b), unequivocally demonstrates that most, if not all, fluorine atoms in **fG** have been replaced by thiophene groups in **fG-Sub** through this simple nucleophilic substitution treatment. Such a high-density addition of thiophene groups in **fG-Sub** is also benefited from the antaratopic addition mode shown in Figure 1b. Hence, considering the wide variety of nucleophiles (*e.g.*, Grignard reagents, amines), one can deliberately control the structure and properties of 2D graphene nanostructures at the nanometer level with high precision.

In summary, a very facile and highly efficient protocol for the covalent 2D-patterning of graphene enabling fine-tuning of its properties has been reported. The patterned fluorination was realized by laser writing on a monolayer graphene coated with 1-fluoro-3,3-dimethylbenziodoxole (solid state reaction) or immersed in the corresponding solution (liquid-phase reaction). This generates highly reactive fluorine radicals exclusively in the irradiated areas, leading to spatially resolved covalent functionalization of graphene. This laser writing process allows not only for a very high degree of functionalization, but also for the realization of sophisticated pattern designs with resolutions down the nanometer level. In addition, by a subsequent substitution with nucleophiles, functional groups otherwise difficult to anchor to the 2D-carbon network can be easily patterned onto graphene with a very high degree of functionalization. This concept was demonstrated in this work where the initially attached electron-withdrawing fluorine atoms have been replaced by electron-donating thiophene groups, leading to a complete switch of both the electronic structure and the polarization within the 2D-functionalized graphene. Considering its simplicity, the nanometer resolution, the very high degree of functionalization, and the numerous possibilities for the substitution, our method provides exciting potentials for the rational fabrication and precise properties tailoring of 2D-structured graphene nanoarchitectures.

Acknowledgements

This work was funded by the Deutsche Forschungsgemeinschaft (DFG, German Research Foundation) - Projektnummer 182849149-SFB 953. Open access funding enabled and organized by Projekt DEAL.

Conflict of Interest

The authors declare no conflict of interest.

Keywords: covalent patterning · fluorination · graphene · polarization switch · substitution

[1] G. Bottari, M. Á. Herranz, L. Wibmer, M. Volland, L. Rodríguez-Pérez, D. M. Guldi, A. Hirsch, N. Martín, F. D'Souza, T. Torres, *Chem. Soc. Rev.* **2017**, *46*, 4464–4500.
[2] Y. Zhu, S. Murali, W. Cai, X. Li, J. W. Suk, J. R. Potts, R. S. Ruoff, *Adv. Mater.* **2010**, *22*, 3906–3924.
[3] C. K. Chua, M. Pumera, *Chem. Soc. Rev.* **2013**, *42*, 3222–3233.
[4] V. Georgakilas, M. Otyepka, A. B. Bourlinos, V. Chandra, N. Kim, K. C. Kemp, P. Hobza, R. Zboril, K. S. Kim, *Chem. Rev.* **2012**, *112*, 6156–6214.
[5] F. M. Koehler, N. A. Luechinger, D. Ziegler, E. K. Athanassiou, R. N. Grass, A. Rossi, C. Hierold, A. Stemmer, W. J. Stark, *Angew. Chem. Int. Ed.* **2009**, *48*, 224–227; *Angew. Chem.* **2009**, *121*, 230–233.
[6] Z. Sun, C. L. Pint, D. C. Marcano, C. Zhang, J. Yao, G. Ruan, Z. Yan, Y. Zhu, R. H. Hauge, J. M. Tour, *Nat. Commun.* **2011**, *2*, 559.
[7] J. Li, M. Li, L.-L. Zhou, S.-Y. Lang, H.-Y. Lu, D. Wang, C.-F. Chen, L.-J. Wan, *J. Am. Chem. Soc.* **2016**, *138*, 7448–7451.
[8] T. Wei, M. Kohring, M. Chen, S. Yang, H. B. Weber, F. Hauke, A. Hirsch, *Angew. Chem. Int. Ed.* **2020**, *59*, 5602–5606; *Angew. Chem.* **2020**, *132*, 5651–5655.
[9] W. H. Lee, J. W. Suk, H. Chou, J. Lee, Y. Hao, Y. Wu, R. Piner, D. Akinwande, K. S. Kim, R. S. Ruoff, *Nano Lett.* **2012**, *12*, 2374–2378.
[10] D. Ye, S.-Q. Wu, Y. Yu, L. Liu, X.-P. Lu, Y. Wu, *Appl. Phys. Lett.* **2014**, *104*, 103105.
[11] K. F. Edelthalhammer, D. Dasler, L. Jurkiewicz, T. Nagel, S. Al-Fogra, F. Hauke, A. Hirsch, *Angew. Chem. Int. Ed.* **2020**, *59*, 23329–23334; *Angew. Chem.* **2020**, *132*, 23529–23534.
[12] L. Bao, M. Kohring, H. B. Weber, F. Hauke, A. Hirsch, *J. Am. Chem. Soc.* **2020**, *142*, 16016–16022.
[13] S. Bian, A. M. Scott, Y. Cao, Y. Liang, S. Osuna, K. N. Houk, A. B. Braunschweig, *J. Am. Chem. Soc.* **2013**, *135*, 9240–9243.
[14] Z. Xia, F. Leonardi, M. Gobbi, Y. Liu, V. Bellani, A. Liscio, A. Kovtun, R. Li, X. Feng, E. Orgiu, P. Samorì, E. Treossi, V. Palermo, *ACS Nano* **2016**, *10*, 7125–7134.
[15] K. Tahara, T. Ishikawa, B. E. Hirsch, Y. Kubo, A. Brown, S. Eyley, L. Daukiya, W. Thielemans, Z. Li, P. Walke, S. Hirose, S. Hashimoto, S. De Feyter, Y. Tobe, *ACS Nano* **2018**, *12*, 11520–11528.
[16] M. Yu, C. Chen, Q. Liu, C. Mattioli, H. Sang, G. Shi, W. Huang, K. Shen, Z. Li, P. Ding, P. Guan, S. Wang, Y. Sun, J. Hu, A. Gourdon, L. Kantorovich, F. Besenbacher, M. Chen, F. Song, F. Rosei, *Nat. Chem.* **2020**, *12*, 1035–1041.
[17] L. Bao, B. Zhao, V. Lloret, M. Halik, F. Hauke, A. Hirsch, *Angew. Chem. Int. Ed.* **2020**, *59*, 6700–6705; *Angew. Chem.* **2020**, *132*, 6766–6771.
[18] L. G. Cançado, A. Jorio, E. H. M. Ferreira, F. Stavale, C. A. Achete, R. B. Capaz, M. V. O. Moutinho, A. Lombardo, T. S. Kulmala, A. C. Ferrari, *Nano Lett.* **2011**, *11*, 3190–3196.
[19] T. Wei, S. Al-Fogra, F. Hauke, A. Hirsch, *J. Am. Chem. Soc.* **2020**, *142*, 21926–21931.
[20] P. Sessi, J. R. Guest, M. Bode, N. P. Guisinger, *Nano Lett.* **2009**, *9*, 4343–4347.
[21] J. Greenwood, T. H. Phan, Y. Fujita, Z. Li, O. Ivasenko, W. Vanderlinden, H. Van Gorp, W. Frederickx, G. Lu, K. Tahara, Y. Tobe, H. Uji-i, S. F. L. Mertens, S. De Feyter, *ACS Nano* **2015**, *9*, 5520–5535.
[22] R. A. Bueno, J. I. Martínez, R. F. Luccas, N. R. del Árbol, C. Munuera, I. Palacio, F. J. Palomares, K. Lauwaet, S. Thakur, J. M. Baranowski, W. Strupinski, M. F. López, F. Mompean, M. García-Hernández, J. A. Martín-Gago, *Nat. Commun.* **2017**, *8*, 15306.
[23] V. Matoušek, E. Pietrasiak, R. Schwenk, A. Togni, *J. Org. Chem.* **2013**, *78*, 6763–6768.
[24] C. Y. Legault, J. Prévost, *Acta Crystallogr. Sect. E Struct. Rep. Online* **2012**, *68*, o1238.
[25] K. Amsharov, D. I. Sharapa, O. A. Vasilyev, M. Oliver, F. Hauke, A. Goerling, H. Soni, A. Hirsch, *Carbon* **2020**, *158*, 435–448.
[26] K. C. Knirsch, R. A. Schäfer, F. Hauke, A. Hirsch, *Angew. Chem. Int. Ed.* **2016**, *55*, 5861–5864; *Angew. Chem.* **2016**, *128*, 5956–5960.
[27] V. Mazánek, O. Jankovský, J. Luxa, D. Sedmidubský, Z. Janoušek, F. Šembera, M. Mikulics, Z. Sofer, *Nanoscale* **2015**, *7*, 13646–13655.
[28] W. Feng, P. Long, Y. Feng, Y. Li, *Adv. Sci.* **2016**, *3*, 1500413.
[29] R. R. Nair, W. Ren, R. Jalil, I. Riaz, V. G. Kravets, L. Britnell, P. Blake, F. Schedin, A. S. Mayorov, S. Yuan, M. I. Katsnelson, H.-M. Cheng, W. Strupinski, L. G. Bulusheva, A. V. Okotrub, I. V. Grigorieva, A. N. Grigorenko, K. S. Novoselov, A. K. Geim, *Small* **2010**, *6*, 2877–2884.
[30] K. E. Whitener, R. Stine, J. T. Robinson, P. E. Sheehan, *J. Phys. Chem. C* **2015**, *119*, 10507–10512.
[31] X. Sun, B. Li, M. Lu, *J. Solid State Chem.* **2017**, *251*, 194–197.
[32] D. D. Chronopoulos, A. Bakandritsos, P. Lazar, M. Pykal, K. Čépe, R. Zbořil, M. Otyepka, *Chem. Mater.* **2017**, *29*, 926–930.

Manuscript received: March 15, 2021
Accepted manuscript online: March 26, 2021
Version of record online: May 1, 2021